

Effects of year-long exposure to elevated pCO₂ on the metabolism of back reef and fore reef communities

Peter J. Edmunds , ^{1*} Steve S. Doo , ^{1,2} Robert C. Carpenter 

¹Department of Biology, California State University, Northridge, California, USA

²Department of Marine Science, University of Hawai'i at Hilo, Hilo, Hawaii, USA

Abstract

The implications of ocean acidification are acute for calcifying organisms, notably tropical reef corals, for which accretion generally is depressed and dissolution enhanced at reduced seawater pH. We describe year-long experiments in which back reef and fore reef (17-m depth) communities from Moorea, French Polynesia, were incubated outdoors under pCO₂ regimes reflecting endpoints of representative concentration pathways (RCPs) expected by the end of the century. Incubations were completed in three to four flumes (5.0 × 0.3 m, 500 L) in which seawater was refreshed and circulated at 0.1 m s⁻¹, and the response of the communities was evaluated monthly by measurements of net community calcification (NCC) and net community productivity (NCP). For both communities, NCC (but not NCP) was affected by treatments and time, with NCC declining with increasing pCO₂, and for the fore reef, becoming negative (i.e., dissolution was occurring) at the highest pCO₂ (1067–1433 μ atm, RCP8.5). There was scant evidence of community adjustment to reduce the negative effects of ocean acidification, and inhibition of NCC intensified in the back reef as the abundance of massive *Porites* spp. declined. These results highlight the risks of dissolution under ocean acidification for coral reefs and suggest these effects will be most acute in fore reef habitats. Without signs of amelioration of the negative effects of ocean acidification during year-long experiments, it is reasonable to expect that the future of coral reefs in acidic seas can be predicted from their current known susceptibility to ocean acidification.

With rising atmospheric partial pressure of carbon dioxide (pCO₂) attributed to anthropogenic activities (IPCC 2018), the potential biological effects of ocean acidification are serious (Riebesell and Gattuso 2015), and already have reduced global seawater pH by 0.1 units since the industrial revolution (Findlay and Turley 2021). The implications of ocean acidification for marine ecosystems are profound (Doney et al. 2009), and are acute for organisms in which the capacity to deposit CaCO₃ is important (Hofmann et al. 2010). As coral reefs rely on the ability of scleractinian corals and other taxa to deposit large quantities of CaCO₃, this ecosystem is uniquely threatened by ocean acidification (Hoegh-Guldberg et al. 2007).

Around the start of the current millennium, a global effort commenced to quantify the impacts of ocean acidification on

corals, coral reef organisms, and coral reef communities (Langdon et al. 2000). The results revealed negative effects of ocean acidification on the net CaCO₃ accretion of a wide range of organisms (Kroeker et al. 2010, 2013), but the responses were more varied for traits like survival, growth, and photosynthesis (Kroeker et al. 2010). In addition to mediating organismal traits, the physiological implications of ocean acidification are evident within micrometer-scale boundary layers around organisms (Cornwall et al. 2013). Within the diffusion boundary layer surrounding photosynthetic organisms, photosynthesis can elevate seawater pH (through sequestering of CO₂) and the carbonate saturation state (Ω), making it easier for calcified taxa to deposit CaCO₃ (Cornwall et al. 2013). This effect is counteracted by respiration, which releases CO₂ to decrease Ω .

In response to appeals for greater ecological relevance in ocean acidification experiments, experiments with corals expanded to include interactive effects (e.g., ocean acidification crossed with temperature), longer incubations under conditions more relevant for coral reef habitats (Dove et al. 2013, 2020), and analyses focusing on coral reef communities on a larger spatial scale (Albright et al. 2016). Experiments conducted with whole reef communities, either in large tanks (Dove et al. 2020; McLachlan et al. 2022), a massive aquarium

*Correspondence: peter.edmunds@csun.edu

Additional Supporting Information may be found in the online version of this article.

Author Contribution Statement: P.J.E. and R.C.C. conceptualized the project and raised funds for its completion. S.D. implemented the experiments in Moorea and conducted primary measurements and analyses. P.J.E., R.C.C., and S.D. interpreted the results. P.J.E. wrote the first draft of the article and conducted the statistical analyses. P.J.E., R.C.C., and S.D. engaged in editing and final writing of the manuscript.

(Langdon et al. 2000), or in situ (Albright et al. 2016), are insightful for understanding how coral reefs will respond to reductions in seawater pH, but they are complex technically to complete. Moreover, the results can be challenging to interpret, as the effects of ocean acidification on the individual organisms do not linearly scale to accurately estimate the effects on the whole ecosystem (Edmunds et al. 2016).

The first experimental analysis of the effects of ocean acidification on a coral reef community was conducted from 1995 to 1999 using a reef composed of Caribbean and Indo-Pacific corals and assembled in a 2650 m³ tank (Langdon et al. 2000). Through additions of HCO_3^- , CO_3^{2-} , and Cl^- , the Ω of seawater was manipulated downwardly with the result that net community calcification (NCC) declined by 40% at an Ω_{arag} of 2.8 that was predicted (in 2000) to occur by 2100 (Langdon et al. 2000). There was no evidence that coral reef organisms acclimated to low Ω_{arag} over days–years (Langdon et al. 2000). Within 5 years of the completion of this study, the sophistication of experimental ocean acidification research with coral reefs increased. Langdon and Atkinson (2005) described an experiment in which two species of Pacific corals were incubated in a 24-m flume in Hawaii to test the effects of seawater flow speed, season (light and temperature), and nutrients on net community productivity (NCP) and NCC. Under these conditions, NCP increased by 22% at an elevated $p\text{CO}_2$ of 789 μatm (in the summer), while NCC declined by 44% (changes were more extreme in the winter). These effects were attributed to stimulation of photosynthesis by elevated $p\text{CO}_2$, and depression of calcification, either by reduced Ω_{arag} , or through competition with photosynthesis for DIC (Langdon and Atkinson 2005).

Dove et al. (2013) established reef communities in 12 tanks (300 L) at Heron Island in 2011, and exposed them to four treatments contrasting historic (104 μatm lower than ambient), present, and future (ambient + 174 and 572 μatm) projected atmospheric $p\text{CO}_2$. In contrast to Langdon and Atkinson (2005), Dove et al. (2013) found no effect of high $p\text{CO}_2$ on NCP, but at the highest $p\text{CO}_2$ (ambient + 572 μatm), daytime calcification was depressed (75% relative to ambient in December), and nighttime dissolution increased (2.7-fold greater than daytime calcification in February). More recently, Dove et al. (2020) extended their studies to an 18-month analysis of the effects of representative concentration pathway (RCP8.5) conditions on reef slope communities (5-m depth) at Heron Island, and tested orthogonal contrasts of ocean acidification and temperature administered as offsets (+ 550 ppm and + 3.5°C, respectively) from ambient conditions. This analysis revealed a strong positive synergy between ocean acidification and thermal bleaching that reduced reef accretion by 77%, and a decoupling of calcifier biomass from the inhibitory effects of ocean acidification on accretion. Changes in the percent cover on benthic surfaces did not reflect the negative implications of ocean acidification for reef-scale carbonate accretion.

Since these early investigations, an increasing number of studies has contributed to this field. They have advanced the

frontier of the field by increasing ecological relevance (e.g., Comeau et al. 2015, 2017), through longer experiments (Carpenter et al. 2018; Edmunds et al. 2020), and by manipulating seawater chemistry on open reefs (Albright et al. 2016), and in partially closed incubations of reef communities (Doo et al. 2019). Among the discoveries has been confirmation of the negative effects of high $p\text{CO}_2$ on NCC (e.g., Albright et al. 2016; Doo et al. 2019), demonstration that these effects are influenced strongly by nighttime dissolution (Doo et al. 2019; Dove et al. 2020), and equivocal evidence of community adjustment to attenuate the effects of ocean acidification (e.g., Comeau et al. 2019 vs. McLachlan et al. 2022). Further, they have revealed a depression in the elevation of the linear relationship between NCP and NCC (but without a change in slope), possibly through competition for DIC between NCP and NCC (Comeau et al. 2017).

The present study describes the results of two, year-long experiments that were conducted in 2015/16 and 2017/18, in which back reef and fore reef communities from Moorea, French Polynesia, were incubated under ambient and three elevated $p\text{CO}_2$ levels. Four dependent variables were measured, NCC (summation of net calcification and dissolution), NCP (net primary production), benthic community structure (percentage cover), and changes in mass (G_{net}) of the taxa in the communities, but the present analyses focus on NCC and NCP. We have described the response of community structure and G_{net} elsewhere (Edmunds et al. 2019a,b; 2020), as well as the metabolic responses of back reef communities to 4 months of treatments (Carpenter et al. 2018). Here, the results for NCC and NCP are used to test three hypotheses: (1) elevated $p\text{CO}_2$ decreases rates of community metabolism (NCC and NCP over diel time scales) for back reef and fore reef communities, (2) there is no community-level adjustment of metabolic responses to elevated $p\text{CO}_2$ over a year, and (3) the organic/inorganic balance of carbon sequestration reflected in the linear relationships between NCP and NCC are unaffected by increasing $p\text{CO}_2$, and are similar for back reef and fore reef communities.

Materials and methods

Common infrastructure

Experiments were conducted in flumes (Supporting Information Fig. S1), consisting of a 5.0 × 0.3 m working section filled to ~ 0.3-m depth with 500 L of seawater (Carpenter et al. 2018, Edmunds et al. 2019a,b; 2020). Four flumes were used for both experiments, but equipment malfunction resulted in one flume being dropped from the analysis of the fore reef communities. See Data S1 for more details.

Communities were exposed to treatments targeting ambient (~ 400 μatm), 700, 1000, and 1300 μatm $p\text{CO}_2$ that approximate atmospheric conditions expected by ~ 2140 under different RCPs (Moss et al. 2010). Experiments began in late Austral spring in 2015 (back reef) and 2017 (fore reef),

and extended 12 months with monthly measurements of community metabolism (this study) and community structure (Edmunds et al. 2019a,b; 2020).

The flumes were filled with seawater pumped from 14-m depth in Cook's Bay and filtered through sand ($\sim 450\text{--}550\text{ }\mu\text{m}$ pore size), and was continuously added to the flumes at 300 L h^{-1} . Seawater was circulated in each flume at 0.1 m s^{-1} using a pump (W. Lim Wave II 373 J s^{-1}), and flow speeds were measured in the working section using a Nortek (Boston, MA) Vectrino Acoustic Doppler Velocimeter. A flow speed of 0.1 m s^{-1} is ecologically relevant to the back reef (Hench et al. 2008), and the fore reef at 15-m depth (Washburn and Moorea Coral Reef LTER 2023).

The seawater was temperature-controlled with chillers that matched the monthly temperatures to the ambient seawater in Cook's Bay. Temperatures were increased from $\sim 27^\circ\text{C}$ in November to $\sim 29^\circ\text{C}$ around April and May, then back to $\sim 27^\circ\text{C}$ the following November. Temperature was recorded using loggers (Onset Hobo Pro 2, $\pm 0.2^\circ\text{C}$) and a certified thermometer ($\pm 0.05^\circ\text{C}$, model 15-077, Fisher Scientific). Sunlight was shaded with neutral density mesh to approximate the light at 2-m depth in the back reef, or 17-m depth on the fore reef, and for the fore reef, blue filters (LEE #183, Lee Filters, Andover, England) were used to simulate light at 17-m depth (see Supporting Information Fig. S2 in Comeau et al. 2016). Photosynthetically active radiation (PAR) was recorded using cosine-corrected loggers (Odyssey, Dataflow Systems, Christchurch, New Zealand), calibrated against a certified Li-Cor cosine sensor ($\pm 5\%$ resolution, LI 192A, Li-Cor, Lincoln, NE, USA) in units of photon flux density (PFD, $\mu\text{mol photons m}^{-2}\text{ s}^{-1}$). Flumes were covered with clear UV-transparent acrylic lids to prevent rain from entering and to reduce wind speed at the air-seawater interface.

The 5-m working section was divided into a central 2.4-m portion and two flanking portions, each 1.3 m in length. The central portion included a 0.3-m deep sediment box that was filled with sediment for the back reef community, but was covered and sealed for the fore reef community where sand accumulations are rare. The sand in the sediment box for the back reef was arranged with a smooth surface, and it lacked the ripples in surface texture that can enhance advective exchange with seawater (Huettel et al. 2014). Members of the benthic community from each habitat were scattered along the working section to create a community composition benchmarked against the empirical benthic community (Edmunds 2024). Community members in the central portion of the flumes were attached to a metal grid and were not removed from the flume so that they could be quantified photographically (Edmunds et al. 2019a,b; 2020). In the flanking portions, community members were removed monthly to measure buoyant weight that was used in the analysis of the ecological responses to treatments. The communities included a few invertebrates (e.g., coral ectosymbionts such as crabs and brittle stars) with herbivores (e.g., sea urchins) to aid in

the control of algae. Routine cleaning (\sim weekly) removed excess algal biomass on the walls and other exposed surfaces of the flumes.

pCO_2 regimes were assigned randomly to the four flumes in each experiment, and the flumes were oriented with their long axis aligned north-south (Supporting Information Fig. S1). Seawater carbonate chemistry was not controlled in the ambient flumes, but in the other three flumes was regulated with CO_2 gas to approach target values. CO_2 was added to the treatment flumes to alter seawater pH relative to a set point (controlled with AquaControllers, Neptune Systems, Morgan Hills, CA) that operated a solenoid to regulate the supply of CO_2 , except in the ambient flume; ambient air was bubbled into all flumes. The system was programmed to apply a nocturnal downward pH adjustment of ~ 0.1 unit to simulate conditions on the reefs of Moorea (Hofmann et al. 2011).

Seawater pH on the total hydrogen scale (pH_T) was measured daily using a hand-held meter (with a DG 115-SC electrode, Mettler Toledo, Columbus, OH, USA) that was calibrated with TRIS buffer (SOP 6a, Dickson et al., 2007). These records were used together with temperature to adjust the pH set points of the AquaController to approach target values. Seawater carbonate chemistry was calculated weekly using pH_T and the total alkalinity (A_T) recorded once during the day and night. A_T was measured using open-cell, acidimetric titrations (SOP 3b, Dickson et al. 2007) with an automatic titrator (T50 Mettler Toledo) operated with a DG 115-SC probe and filled with certified acid (A. Dickson, Scripps Institute of Oceanography [SIO]). The accuracy and precision of the analyses were determined from reference materials (CRMs, batches 158 and 172, A. Dickson, SIO). Relative to CRMs, determinations of A_T maintained an accuracy of $1.7 \pm 0.3\text{ }\mu\text{mol kg}^{-1}$ to $2.7 \pm 0.4\text{ }\mu\text{mol kg}^{-1}$, and a precision of $1.8 \pm 0.1\text{ }\mu\text{mol kg}^{-1}$ ($n = 475$). Calculations to determine seawater carbonate chemistry were made using temperature, salinity, and pH_T , in the R package Seacarb (Lavigne and Gattuso 2013).

Calculations of benthic metabolism

Community metabolism was assessed using NCC and net community productivity (NCP) that were calculated using the alkalinity anomaly method (Eq. 1 after Smith 1973), and changes in dissolved oxygen (DO see Data S1) (for NCP, Eq. 2):

$$\text{NCC} = \frac{-0.5\Delta A_T V_\rho}{\Delta t \text{SA}} \quad (1)$$

$$\text{NCP} = \frac{\Delta \text{DO} V_\rho}{\Delta t \text{SA}} \quad (2)$$

where ΔA_T is the change in A_T ($\mu\text{mol kg}^{-1}$), V is the volume of the seawater in the flumes (L), ρ is seawater density (kg L^{-1}), Δt is the duration of incubation, SA is the planar area of the floor of the flumes (m^2), and DO is the change in dissolved O_2 concentration ($\mu\text{mol kg}^{-1}\text{ h}^{-1}$).

NCC and NCP were measured under ambient conditions in all flumes at the start of the experiments, the $p\text{CO}_2$ treatments were initiated, and NCC and NCP again were measured. For the back reef community, NCC and NCP were measured biweekly or monthly for the first 4 months (to March 2016) and then monthly until the end of the experiment. Single measurements every month revealed variance attributed to weather and, therefore for the fore reef community, NCC and NCP were recorded on 3 days every month, with the 3 days usually consecutive. Each day of measurements consisted of six determinations, two in the morning (06:00–09:00 h and 09:00–12:00 h), two in the afternoon (12:00–15:00 h and 15:00–18:00 h), and two at night (18:00–24:00 h and 24:00–06:00 h). These times were accurately recorded, but each period varied to accommodate logistical constraints. Each determination was completed with the flumes operating in closed-circuit mode, during which the inflow of fresh seawater was halted. The flumes were flushed for ~ 30 min between each incubation by re-initiating the inflow of seawater at $\sim 5 \text{ L min}^{-1}$, thereby exchanging ~ 25 –30% of the seawater between incubations.

For the back reef community, for which a single day of measurements was obtained monthly, missing values were interpolated using a third order polynomial (for NCC) or a fourth order polynomial (NCP) for empirical values against time of day (Carpenter et al. 2018). NCC and NCP were calculated as hourly rates ($\text{mmol CaCO}_3 \text{ m}^{-2} \text{ h}^{-1}$ and $\text{mmol O}_2 \text{ m}^{-2} \text{ h}^{-1}$, respectively) with positive values reflecting net CaCO_3 accretion and a net release of photosynthetically fixed O_2 , and negative values reflecting net dissolution of CaCO_3 and a net uptake of O_2 , all respectively. NCC was integrated over the day and night to gain insight into the relative effects of treatment on carbonate accretion (that occurs mostly during the day) vs. dissolution (that occurs mostly at night) (Dove et al. 2013; 2020), and NCP was integrated over the day to evaluate net primary production. Local day length was used to calculate day and night rates, with day length varying from 13:17 h in December to 11:08 h in June.

Back reef experiment, 2015–2017

The back reef experiment began in November 2015 (Edmunds et al. 2019a,b), and the communities were assembled to mimic the community found in the back reef of Moorea in 2013 (Edmunds 2024). Community members were collected from ~ 2 -m depth on the north shore. Initially, the communities had $\sim 25\%$ coral cover with 11% massive *Porites* spp., 7% *P. rus*, 4% *Montipora* spp., 3% *Pocillopora* spp., and $\sim 7\%$ crustose coralline algae (CCA) with 4% *Porolithon onkodes*, and 3% *Lithophyllum kotschyani*. Corals and CCA were attached to plastic bases (using Z-Spar A788). Coral rubble (~ 1 -cm diameter) was added to $\sim 5\%$ cover, and the remainder of the floor of the flume was sand. Communities were assembled on top of the sand and were augmented with a few holothurians (~ 8 -cm long, *Holothuria* spp.) and macroalgae (*Turbinaria ornata* and

Halimeda minima) that were added to ecologically relevant cover for the back reef in 2013 (~ 4 –5% cover). The communities were established in the flumes by 12 November 2015, and were maintained under ambient $p\text{CO}_2$ for 5 d until $p\text{CO}_2$ treatments were established in three flumes; $p\text{CO}_2$ was increased over 24 h to establish target values.

Fore reef experiment, 2017–2018

The fore reef experiment began in November 2017 (Edmunds et al. 2020), and communities were assembled in the flumes to mimic the community found at 17-m depth on the fore reef of Moorea in 2006 (Carpenter 2023; Edmunds 2024). An historic community was used as a target because it better reflected the long-term representative fore reef community in this location (Edmunds et al. 2019b), and because it allowed a more direct comparison with previous short-term incubations completed with fore reef communities (Comeau et al. 2016). Community members were collected from 17-m depth on the north shore fore reef. Initially, the communities had $\sim 27\%$ coral cover with $\sim 11\%$ *Pocillopora* spp., $\sim 8\%$ massive *Porites* spp., $\sim 8\%$ *Acropora* spp. and 53% reef rock. The *Pocillopora* conformed to *P. verrucosa* (after Veron 2000), but multiple species probably were present (Burgess et al. 2021). Likewise, the *Acropora* spp. targeted *A. hyacinthus* and *A. retusa*, which are common on the fore reef of Moorea (Comeau et al. 2014), but possibly included other species. Corals were attached to plastic bases (with Z-Spar A788). The reef rock consisted of rubble (~ 12 -cm diameter) and the flora and fauna with which it was associated. The communities were established in the flumes by 27 October 2017 and were maintained under ambient $p\text{CO}_2$ for 7 d, when the $p\text{CO}_2$ treatments were initiated over 24 h to reach target values. Because of equipment malfunctions, the fore reef experiment was completed with 3 flumes that targeted ambient conditions 400, 700, and $1300 \mu\text{atm}$ $p\text{CO}_2$.

Statistical analysis

NCC and NCP were analyzed separately for each experiment, and in both cases, linear, mixed-effects models were fitted using restricted maximum likelihood (REML) methods, in which treatments ($p\text{CO}_2$ regimes) and time (i.e., measurement day) were fixed effects (covariates), and light, temperature, and coral cover were random covariates. Four analyses were conducted for each experiment, with each employing a different dependent variable (24 h-NCC, day-NCC, night-NCC, and NCP). For the fore reef experiment, the three measurements month $^{-1}$ were averaged to provide a single value for each month to facilitate a contrast with the back reef experiment. To evaluate changes in metabolism over time, the average of the monthly measurements was registered against the second of the three-day measurement sequence. Light was integrated over a day ($\text{mol photons m}^{-2} \text{ d}^{-1}$) on the day that community metabolism was measured (back reef), or was averaged over the three measurement periods (fore reef). Temperature was the mean daily temperature over the month preceding the

metabolism measurements, and coral cover was calculated from planar photographs (as in Edmunds et al. 2019a,b; 2020).

To understand the integrative balance between inorganic (NCC) and organic (NCP) carbon sequestration, the relationships between NCC and NCP (by hour) were explored using scatter plots, with associations tested using Pearson correlations. Linear relationships were displayed using Model I regressions. To test for variation in NCC–NCP relationships over time, the slopes and elevations of the NCC–NCP relationships were compared among seasons using ANCOVA. The seasonal contrast was created by segregating results from November–February (near Austral summer), March–May (near austral autumn), June–August (near Austral winter), and September–November (near Austral spring).

To test for linear relationships between 24 h-NCC and $p\text{CO}_2$, Model I linear regressions were fit to the results by month ($n = 3\text{--}4$ $p\text{CO}_2$ treatments) using the single measure month $^{-1}$ for the back reef experiment, and the 3 measures month $^{-1}$ for the fore reef experiment. To test for variation over time (year) in the sensitivity of the 24 h, NCC– $p\text{CO}_2$ relationship, Model I linear regression was used, in which the slopes of the 24 h-NCC– $p\text{CO}_2$ relationships by time were the dependent variable, and the independent variable was time (days over the incubation year).

Statistical analyses were completed using Systat 13.0 software (Inpixon, Palo Alto, USA), and the statistical assumptions of ANOVA were tested using graphical analysis of residuals.

Results

Overview

Both experiments maintained the treatments conditions, although year-long mean $p\text{CO}_2$ regimes departed from a priori target values. Treatment conditions for all flumes in both experiments are summarized in Supporting Information Table S1 and Fig. S2. In the back reef experiment, mean $p\text{CO}_2$ treatments contrasted $363 \pm 32 \mu\text{atm}$ (ambient), $564 \pm 26 \mu\text{atm}$, $762 \pm 16 \mu\text{atm}$, and $1067 \pm 49 \mu\text{atm}$ ($\pm \text{SE}$, $n = 8\text{--}12$) and when the experiment began in November 2015, these flumes contained 27%, 25%, 26%, and 27% coral cover (respectively). When the experiment ended, they contained 22%, 20%, 24%, and 22%, respectively (all values in November 2016, except for the 762 μatm flume that malfunctioned after July 2016) (Fig. 1). In the fore reef experiment, mean $p\text{CO}_2$ treatments contrasted $396 \pm 11 \mu\text{atm}$ (ambient), $782 \pm 18 \mu\text{atm}$, and $1433 \pm 24 \mu\text{atm}$ ($\pm \text{SE}$, $n = 12$), and when the experiment began in November 2017, these three flumes contained 18%, 20%, and 18% coral cover (respectively). When the experiment ended, they contained 11%, 13%, and 13% respectively (all values in November 2018) (Fig. 1).

Back reef experiment, 2015–2017

Community metabolism varied among months, especially in the ambient flume (Fig. 2, Supporting Information Fig. S2). In the ambient $p\text{CO}_2$ flume, 24 h-NCC ranged between

66 mmol $\text{CaCO}_3 \text{ m}^{-2} 24 \text{ h}^{-1}$ (February 2016) and 134 mmol $\text{CaCO}_3 \text{ m}^{-2} 24 \text{ h}^{-1}$ (November 2016) and trended upwards over the year, with the final value 46% greater than the initial value. Day-NCC and night-NCC showed similar trends, with final values 44% and 53% greater than the initial values (respectively), with no cases of net dissolution (i.e., $\text{NCC} \geq 0$ over the whole year). NCP ranged from 12 mmol $\text{O}_2 \text{ m}^{-2} \text{ d}^{-1}$ (October 2016) to 70 mmol $\text{O}_2 \text{ m}^{-2} \text{ d}^{-1}$ (March 2016), and while it varied among months, the final value was 48% higher than the initial value (Supporting Information Fig. S3).

Among-month variation in NCC was attenuated (relative to the control) in the three flumes at elevated $p\text{CO}_2$, with mean 24 h-NCC (averaged over the whole year) reduced by 25% (564 μatm , $n = 15$), 42% (762 μatm , $n = 11$), and 54% (1067 μatm , $n = 15$). Overall, day-NCC was reduced less (16%, 33%, and 44%, respectively) than night-NCC (61%, 78%, and 91%, respectively) (Fig. 1); NCP showed only small changes among treatments, increasing 6%, 8%, and 15%, respectively (Supporting Information Fig. S3) (all averaged over the experiment).

In the 564 μatm flume, 24 h-NCC ranged from 56 mmol $\text{CaCO}_3 \text{ m}^{-2} 24 \text{ h}^{-1}$ (November 2015) to 98 mmol $\text{CaCO}_3 \text{ m}^{-2} 24 \text{ h}^{-1}$ (July 2016) and increased over time with the final value 11% greater than the initial value. Day-NCC and night-NCC showed similar trends, and net dissolution was recorded at night in 1 month (March 2016). In the 762 μatm flume (that was operated to July 2016), 24 h-NCC ranged from 33 mmol $\text{CaCO}_3 \text{ m}^{-2} 24 \text{ h}^{-1}$ (January 2015) to 99 mmol $\text{CaCO}_3 \text{ m}^{-2} 24 \text{ h}^{-1}$ (July 2016) and increased over time with the final value 53% greater than the initial value. Day-NCC and night-NCC showed similar trends, and net dissolution was recorded at night in 2 months (January and March 2016). In the 1067 μatm flume, 24 h-NCC ranged from 19 mmol $\text{CaCO}_3 \text{ m}^{-2} 24 \text{ h}^{-1}$ (April 2015) to 87 mmol $\text{CaCO}_3 \text{ m}^{-2} 24 \text{ h}^{-1}$ (July 2016), and increased over time with the final value 27% greater than the initial value. Day-NCC and night-NCC showed similar trends, and net dissolution was recorded at night in six months (February–April, June, September, and November 2016). As recorded in the ambient flume, NCP varied among months, and the final values were greater than initial values in the 564 μatm and 762 μatm flumes, but not in the 1067 μatm flume (Supporting Information Fig. S3).

The mixed-model analyses revealed significant effects of $p\text{CO}_2$ on 24 h-NCC, day-NCC, and night-NCC, but not on NCP, and significant effects of time on 24 h-NCC and day-NCC (but not night-NCC or NCP) (Table 1). Analyses of estimates for these fixed effects showed that 24 h-NCC, day-NCC and night-NCC declined with increasing $p\text{CO}_2$, and both 24 h-NCC and day-NCC increased over time. Analysis of the random covariates showed that day-NCC and NCP increased with daily-integrated PFD, but no other effects of the random covariates were detected (Table 1).

The relationships between hourly NCC and NCP were significant ($r \geq 0.581$, $n = 63\text{--}87$, $p \leq 0.001$) and positive for all

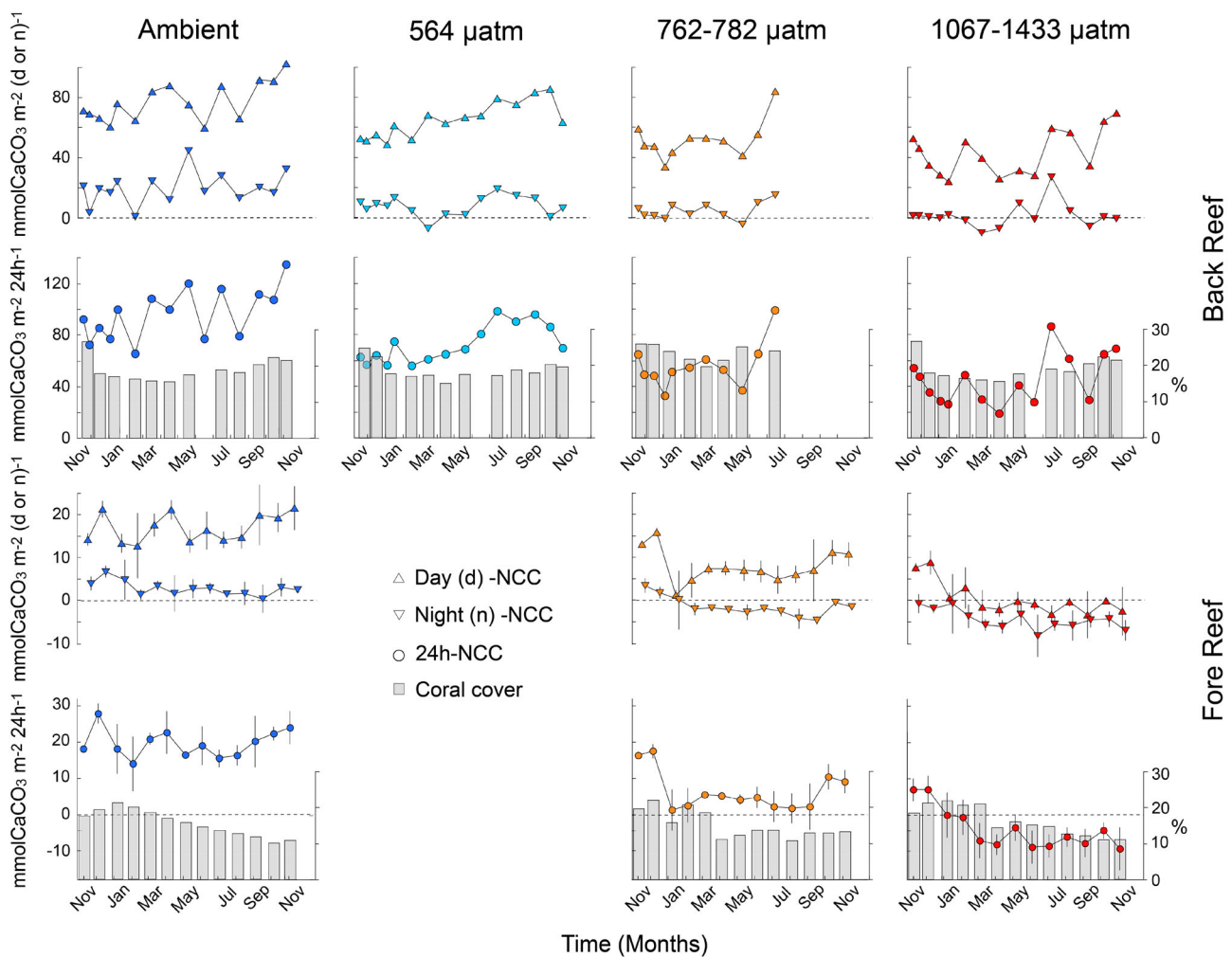


Fig. 1. NCC and coral cover for back reef (top row) and fore reef (bottom row) communities exposed to three to four treatments over a year in 2015–2016 or 2017–2018. NCC is plotted against day of measurement on a continuously distributed time axis, but coral cover is plotted by month. NCC displayed for daytime (Day-NCC) and nighttime (Night-NCC) (both right ordinates) and for the whole day (24 h-NCC, the sum of Day-NCC and Night-NCC, left ordinate), with Day-NCC and Night-NCC adjusted to reflect variation in day lengths throughout the year. Single incubation values are plotted for the back reef, but mean \pm SE ($n = 3$ d) are plotted for the fore reef. Single values for coral cover (left outer ordinate) are plotted for both communities.

flumes, with slopes of $0.196 \text{ mmol CaCO}_3 \text{ m}^{-2} \text{ h}^{-1}$ ($\text{mmol O}_2 \text{ m}^{-2} \text{ h}^{-1}\right)^{-1}$ (ambient), $0.212 \text{ mmol CaCO}_3 \text{ m}^{-2} \text{ h}^{-1}$ ($\text{mmol O}_2 \text{ m}^{-2} \text{ h}^{-1}\right)^{-1}$ ($564 \mu\text{atm}$), $0.201 \text{ mmol CaCO}_3 \text{ m}^{-2} \text{ h}^{-1}$ ($\text{mmol O}_2 \text{ m}^{-2} \text{ h}^{-1}\right)^{-1}$ ($762 \mu\text{atm}$), and $0.179 \text{ mmol CaCO}_3 \text{ m}^{-2} \text{ h}^{-1}$ ($\text{mmol O}_2 \text{ m}^{-2} \text{ h}^{-1}\right)^{-1}$ ($1067 \mu\text{atm}$) (Fig. 2). The slopes of these relationships did not differ among treatments ($F_{3,316} = 1.381, p = 0.833$), but the relationships varied in elevation among treatments ($F_{3,316} = 19.465, p < 0.001$). The elevations in all pCO_2 treatments were depressed relative to the ambient flume ($p \leq 0.008$), and were lower at $1067 \mu\text{atm}$ compared to $761 \mu\text{atm}$ ($p < 0.001$). When the NCP-NCC relationships were separated by time over the year using four blocks approximating seasons (color-coding in Fig. 2), the slopes and elevations were similar among the four seasons (Supporting Information Fig. S4).

The relationships between 24 h-NCC and pCO_2 yielded 14 slopes for which the least squares linear regressions explained 41–99% of the variance (Supporting Information Table S2); with sample sizes of three to four, only three of the relationships were statistically significant. The slopes varied among times (Fig. 3a), and ranged from $-0.017 \text{ mmol CaCO}_3 \text{ m}^{-2} 24 \text{ h}^{-1} \mu\text{atm}^{-1}$ (15 January 2016) to $-0.127 \text{ mmol CaCO}_3 \text{ m}^{-2} 24 \text{ h}^{-1} \mu\text{atm}^{-1}$ (15 April 2016). There was no significant relationship between these slopes and time ($F_{1,12} = 0.527, p = 0.482$).

Fore reef experiment, 2017–2018

Community metabolism varied among months, especially in the ambient flume (Fig. 2, Supporting Information Fig. S2), but the variation was less pronounced than for the back reef.

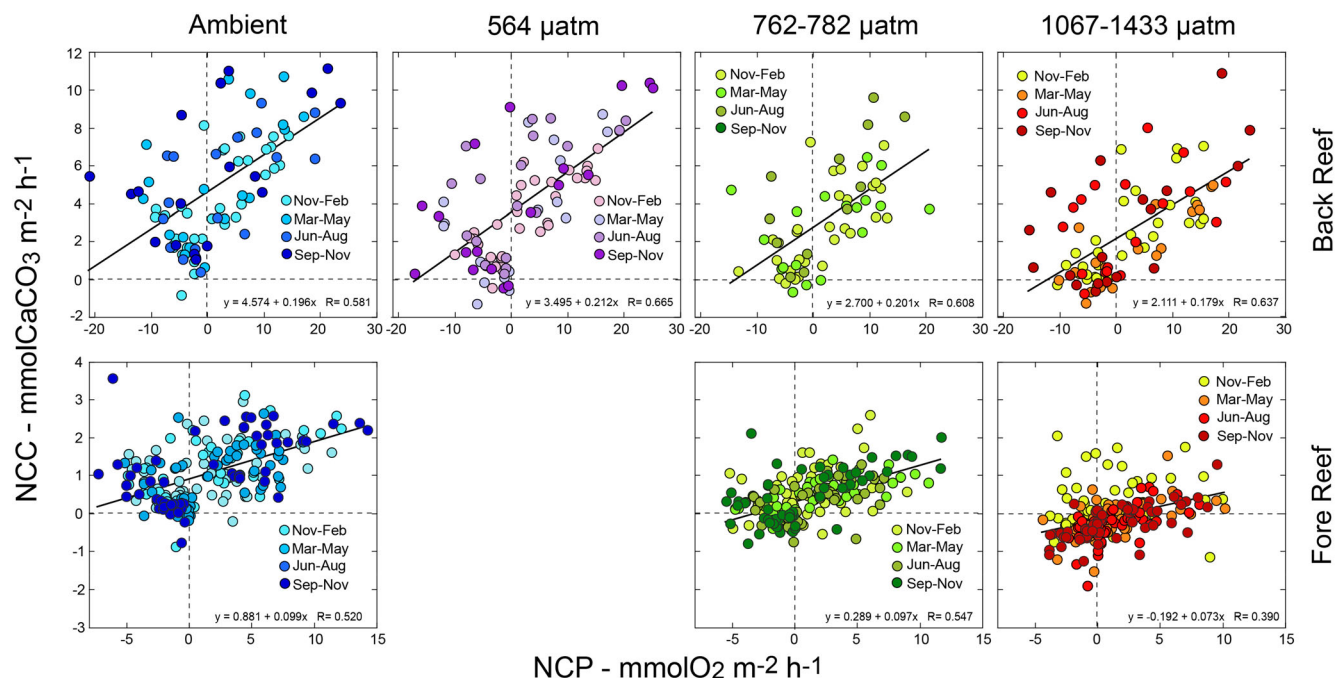


Fig. 2. NCC vs. NCP that were calculated for each analytical determination for back reef (top row) and fore reef (bottom row) using values from year-long incubations under three or four treatment conditions. Six measurements were made each day, two in the morning, two in the afternoon, and two at night, and measurements were made 1 d month $^{-1}$ for the back reef and 3 d month $^{-1}$ for the fore reef. Symbols are color coded for each experiment to reflect four seasonal phases of the experiment, November–February, March–May, June–August, and September–November. Straight lines are best-fit least squares linear regressions.

Under ambient $p\text{CO}_2$, 24 h-NCC ranged between 14.0 $\text{mmol CaCO}_3 \text{ m}^{-2} 24 \text{ h}^{-1}$ (February 2018) and 27.9 $\text{mmol CaCO}_3 \text{ m}^{-2} 24 \text{ h}^{-1}$ (December 2017) and trended upwards over the year, with the final value 32% greater than the initial day. Day-NCC also trended upwards, with the final value 51% greater than the initial value, but night-NCC trended downwards, with the final value 36% lower than the initial value. None of the NCC values indicated net dissolution (i.e., all were $\geq 0 \text{ mmol CaCO}_3 \text{ m}^{-2} 24 \text{ h}^{-1}$). NCP increased over time (Supporting Information Fig. S3), and the final value was 271% greater than the initial value. All aspects of community metabolism under ambient conditions were reduced for the fore reef compared to the back reef community, with 24 h-NCC reduced by 80%, day-NCC by 78%, night-NCC by 86%, and NCP by 36% (based on values averaged over the year).

Among-month variation in NCC generally was attenuated in the two flumes at elevated $p\text{CO}_2$, except for the large reduction in 24 h-NCC and day-NCC between December and January in the 782 μatm flume. Mean 24 h-NCC was reduced by 68% at 782 μatm , and indicated net dissolution at 1433 μatm . Day-NCC was reduced by 53% at 782 μatm) and 99.7% at 1433 μatm , and night-NCC transitioned to net dissolution at 782 μatm , and net dissolution increased by 293% at 1433 μatm (Fig. 1). NCP showed relative small changes among flumes, and declined by 31% at 782 μatm , and by 24% at

1433 μatm (Supporting Information Fig. S3) (all averaged over the experiment).

In the 782 μatm flume, mean 24 h-NCC ranged from 1.2 $\text{mmol CaCO}_3 \text{ m}^{-2} 24 \text{ h}^{-1}$ (January 2018) to 17.5 $\text{mmol CaCO}_3 \text{ m}^{-2} 24 \text{ h}^{-1}$ (December 2017), and trended downward over time, with the final value 44% lower than the initial value. Day-NCC and night-NCC showed similar trends, with the final mean day-NCC reduced by 18% compared to the initial value, and mean night-NCC becoming negative in February 2018, and remaining negative for the remainder of the year (Fig. 1). In the 1433 μatm flume, mean 24 h-NCC ranged from 7.1 $\text{mmol CaCO}_3 \text{ m}^{-2} 24 \text{ h}^{-1}$ (December 2017) to $-9.4 \text{ mmol CaCO}_3 \text{ m}^{-2} 24 \text{ h}^{-1}$ (November 2018), and rapidly declined over time to end the experiment with a high rate of net dissolution. Day-NCC and night-NCC showed similar trends, with both indicating net dissolution by March 2018, which persisted for the remainder of the year. As recorded in the ambient flume, mean NCP in the 782 μatm and 1433 μatm flumes trended upwards over the year, with final rates 291% or 225% higher than initial values (Supporting Information Fig. S3).

The mixed model analyses revealed significant effects of $p\text{CO}_2$ on 24 h-NCC, day-NCC, and night NCC, but not on NCP, and significant effects of time on 24 h-NCC and night-NCC (but not day-NCC or NCP) (Table 1). Analyses of estimates for these fixed effects showed that 24 h-NCC, day-NCC

Table 1. Results of mixed model analyses in which four aspects of community metabolism were used as dependent variables, treatment ($p\text{CO}_2$), and time (days throughout the year-long incubations) were considered fixed effects (covariates), and temperature ($^{\circ}\text{C}$), light (PFD integrated over the measurement day), coral cover (percentage, determined concurrently with metabolism measurements) were considered as random covariates. Models were fit using REML methods. DV = dependent variable.

Experiment	DV	Effect	Estimate	Lower 95% CI	Upper 95% CI	Type III tests of fixed effects
Back reef	24 h-NCC	Treatment	-0.075	-0.092	-0.059	$F_{1,42} = 86.415, p < 0.001$
		Time	0.109	0.065	0.152	$F_{1,42} = 25.720, p < 0.001$
		Temperature	0.000	-0.001	0.001	
		Light	0.502	-0.103	1.106	
		Coral cover	0.000	-0.001	0.001	
	Day-NCC	Treatment	-0.051	-0.061	-0.040	$F_{1,42} = 91.965, p < 0.001$
		Time	0.090	0.062	0.119	$F_{1,42} = 41.663, p < 0.001$
		Temperature	0.000	-0.001	0.001	
		Light	0.346	0.054	0.745	
		Coral cover	0.000	-0.001	0.001	
Night-NCC	Night-NCC	Treatment	-0.023	-0.033	-0.012	$F_{1,42} = 19.814, p < 0.001$
		Time	0.016	-0.011	0.042	$F_{1,42} = 1.444, p = 0.236$
		Temperature	0.000	-0.002	0.002	
		Light	0.006	-0.066	0.079	
		Coral cover	0.279	-0.281	0.839	
	NCP	Treatment	0.004	-0.012	0.020	$F_{1,42} = 0.269, p = 0.606$
		Time	-0.034	-0.074	0.006	$F_{1,42} = 2.995, p = 0.091$
		Temperature	0.189	-1.172	1.550	
		Light	1.889	1.277	2.502	
		Coral cover	0.829	-1.839	0.182	
Fore reef	24 h-NCC	Treatment	-0.028	-0.032	-0.024	$F_{1,30} = 215.744, p < 0.001$
		Time	-0.035	-0.062	-0.009	$F_{1,30} = 7.383, p = 0.011$
		Temperature	-6.332	-9.398	-3.266	
		Light	0.000	0.000	0.000	
		Coral cover	0.201	-0.302	0.705	
	Day-NCC	Treatment	-0.020	-0.023	-0.016	$F_{1,30} = 160.579, p < 0.001$
		Time	-0.018	-0.038	0.002	$F_{1,30} = 3.455, p = 0.073$
		Temperature	-3.990	-6.430	-1.551	
		Light	0.000	0.000	0.000	
		Coral cover	0.101	-0.236	0.437	
	Night-NCC	Treatment	-0.008	-0.010	-0.007	$F_{1,30} = 149.297, p < 0.001$
		Time	-0.020	-0.027	-0.013	$F_{1,30} = 34.090, p < 0.001$
		Temperature	-2.314	-3.402	-1.226	
		Light	0.000	0.000	0.000	
		Coral cover	0.001	-0.026	0.029	
	NCP	Treatment	-0.007	-0.017	0.002	$F_{1,30} = 2.600, p = 0.117$
		Time	-0.001	-0.061	0.059	$F_{1,30} = 0.002, p = 0.968$
		Temperature	-3.566	-9.507	2.376	
		Light	0.000	-0.001	0.001	
		Coral cover	-0.514	-1.753	0.725	

and night-NCC declined with increasing $p\text{CO}_2$, and both 24 h-NCC and day-NCC declined over time. Analysis of the random covariates showed that 24 h-NCC, day-NCC, and night NCC were strongly affected by temperature, and all

declined with warmer temperatures; no other effects of the random covariates were detected (Table 1).

The relationships between NCP and NCC were significant ($r \geq 0.390, n = 228, p < 0.001$) and positive for all flumes, with

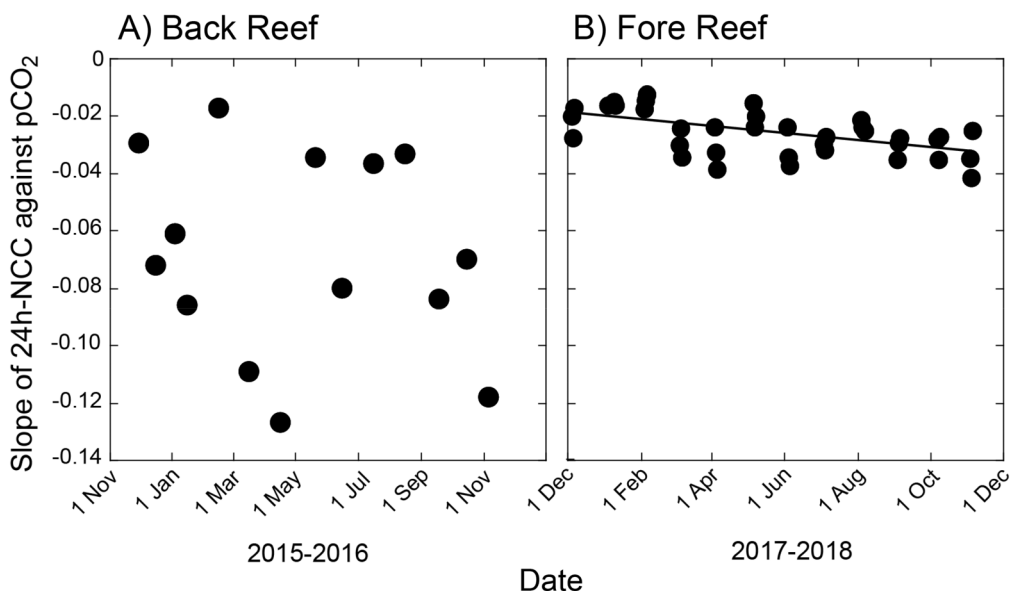


Fig. 3. Slopes of least squares linear regressions (Supporting Information Table S2) of 24 h-NCC against $p\text{CO}_2$ (Supporting Information Table S1) on the day of measurement for the back reef (a) and fore reef (b) over 2015–2016 or 2017–2018, respectively. Slopes are based on three to four determinations (Supporting Information Table S1) and they become steeper over time for fore reef, but not back reef communities.

slopes of $0.099 \text{ mmol CaCO}_3 \text{ m}^{-2} \text{ h}^{-1}$ ($\text{mmol O}_2 \text{ m}^{-2} \text{ h}^{-1}$) $^{-1}$ (ambient), $0.097 \text{ mmol CaCO}_3 \text{ m}^{-2} \text{ h}^{-1}$ ($\text{mmol O}_2 \text{ m}^{-2} \text{ h}^{-1}$) $^{-1}$ ($782 \mu\text{atm}$) and $0.073 \text{ mmol CaCO}_3 \text{ m}^{-2} \text{ h}^{-1}$ ($\text{mmol O}_2 \text{ m}^{-2} \text{ h}^{-1}$) $^{-1}$ ($1433 \mu\text{atm}$) (Fig. 2). The slopes of these relationships did not vary among treatments ($F_{2,678} = 1.593$, $p = 0.204$), but the relationships differed in elevation among treatments ($F_{1,678} = 176.445$, $p < 0.001$); all combinations of elevations differed ($p < 0.001$), and decreased from ambient to $782 \mu\text{atm}$ and to $1433 \mu\text{atm}$ (Fig. 2). When the NCC–NCP relationships were separated by time over the year using four blocks approximating seasons (color-coding in Fig. 2), the slopes and elevations were similar among seasons (Supporting Information Fig. S4).

The relationships between 24 h-NCC and $p\text{CO}_2$ on the days of measurement throughout the year yielded 36 slopes for which the least squares linear regressions explained 61%–99% of the variance (Supporting Information Table S2); with sample sizes of three, six of the relationships were statistically significant. The slopes were more consistent along times compared to the back reef (Fig. 3), and ranged from $-0.014 \text{ mmol CaCO}_3 \text{ m}^{-2} 24 \text{ h}^{-1} \mu\text{atm}^{-1}$ (4 February 2018) to $-0.041 \text{ mmol CaCO}_3 \text{ m}^{-2} 24 \text{ h}^{-1} \mu\text{atm}^{-1}$ (4 November 2018). The slope of these relationships declined over time ($F_{1,34} = 14.566$, $p = 0.001$).

Discussion

Our study achieves ecological relevance in understanding how coral reefs will be affected by ocean acidification by: (1) conducting year-long experiments outdoors, (2) working with reef communities composed of coral reef biota, sediment,

and rubble, at densities benchmarked against two reef habitats, and (3) conducting incubations at $p\text{CO}_2$ values representing RCPs (i.e., from 2.6, strong mitigation, to 8.5, most severe scenario) that are feasible for the next century (Moss et al. 2010), and (4) maintaining seawater flow conditions commonly experienced by benthic communities in situ.

Hypothesis 1: High $p\text{CO}_2$ affects community metabolism Effects of ocean acidification on NCC

Elevated $p\text{CO}_2$ had negative effects on day-NCC, night-NCC, and 24 h-NCC for back reef and fore reef communities, and fore reef NCC was lower and more stable than back reef NCC. For the fore reef, day-NCC transitioned to dissolution within ~ 4 months at $1433 \mu\text{atm}$ $p\text{CO}_2$, night-NCC transitioned to dissolution within 3 months at 782 and $1433 \mu\text{atm}$ $p\text{CO}_2$, and 24 h-NCC transitioned to dissolution within 4 months at $1433 \mu\text{atm}$ $p\text{CO}_2$ (Fig. 1). For the back reef, 24 h-NCC remained positive regardless of $p\text{CO}_2$ and, therefore, did not transition into dissolution during the year incubation (Fig. 1). The results from our fore reef incubations corroborate predictions that NCC of coral reefs could transition from net accretion to dissolution within ~ 100 years (Andersson and Gledhill 2013; Dove et al. 2020) depending on the ability of humans to curtail CO_2 emissions. Our experiments indicate that the structural integrity of shallow coral reefs may be challenged by ocean acidification through framework dissolution amplified on the fore reef, with this effect masked by limited consequences for calcifier biomass (sensu Dove et al. 2020) and the resilience of benthic community structure to elevated $p\text{CO}_2$ (Edmunds et al. 2019a,b; 2020).

Previous studies have reported trends toward net dissolution of coral reefs by the end of the century as a result of ocean acidification, both for specific reefs with well-developed sediment communities (Eyre et al. 2018), and for results from numerous reefs in a synthetic analysis (Cornwall et al. 2021). While decreased NCC under ocean acidification in the present study (Fig. 1) is probably a result of low pH and high $p\text{CO}_2$ reducing physiological performances, in future warmer and more acidic seas it is likely that coral reef NCC will also be depressed through the bleaching-induced death of corals (Dove et al. 2020; Cornwall et al. 2021). In our flumes, bleaching did not appear to contribute to the declines in NCC, because any mortality of coral colonies occurred within the first few months (Autumn), and paling of coral colonies during the hottest months was not observed (S. Doo personal observation). Moreover, our results indicate that ocean acidification elicits an immediate inhibitory response of NCC (e.g., Comeau et al. 2019), which together with the interactive effects of ocean acidification with light and temperature on metabolism (Dove et al. 2020), can explain why NCC integrated by day, night, and 24 h, differed among months (Supporting Information Table S1) for both communities (except night-NCC for the back reef). Ultimately, the rapidity with which coral reef NCC responds negatively to ocean acidification explains the dynamic and temporally inconsistent variation of this state variable to monthly environmental conditions (Fig. 1).

Effects of ocean acidification on NCP

Because NCP was unaffected by $p\text{CO}_2$, our results do not support the notion of ecologically meaningful “fertilization” of photosynthesis by high $p\text{CO}_2$ (Kroeker et al. 2010, 2013). Instead, they indicate that ocean acidification does not alter primary production over a year. This conclusion is consistent with the role of light (PFD) underlying the short-term variation in the NCP of shallow coral reefs (Takashita et al. 2016). In our experiments, PFD varied among days differing in cloud cover, and seasonal variation was prominent when the back reef communities were incubated (over 2015–2016), but not when the fore reef were incubated (over 2017–2018) (Supporting Information Fig. S1).

Hypothesis 2: Community adjustment to ocean acidification

The capacity of coral communities to adjust to ocean acidification is critical information in efforts to evaluate the long-term implications of this stressor (Hofmann et al. 2010). Adjustment might involve reorganization of the organic and inorganic components of coral communities, and could occur through physiological acclimatization (Fantazzini et al. 2015), epigenetic effects (Putnam et al. 2016), changes in the taxa combined within the holobiont (Camp et al. 2020), or adaptation (Schoepf et al. 2017). To be effective, these hypothesized mechanisms would also need to address the energetic tradeoffs inherent in the calcification process vs. the metabolic costs of homeostasis

with respect to declining seawater pH (Clark 2020). For coral calcification, these are likely to focus on the metabolic cost of modifying the pH of calcifying fluid between the coral tissue and the skeleton surface (Comeau et al. 2017).

Evidence of phenotypic adjustments in response to ocean acidification in reef corals remains scant (Comeau et al. 2019; but see McLachlan et al. 2022), and signs that corals can adapt genetically to reduced pH remains equivocal (Schoepf et al. 2017; Dove et al. 2020). Confronted with the speed and magnitude of changes in seawater chemistry that is projected to occur through ocean acidification, it is more feasible that reef communities might adjust their sensitivity to reduced seawater pH through changes in the abundance of resistant vs. sensitive taxa (Comeau et al. 2014). Substitution of pH-sensitive species (like *Psammocora profundacella* (Comeau et al. 2014) for pH-resistant species (*Pocillopora verrucosa*; Comeau et al. 2014), would reduce the overall sensitivity of the coral community to ocean acidification. More nuanced effects could arise through changes in abundance of non-calcified macroalgae that could alter seawater pH through their metabolism (Doo et al. 2020), or variation in inorganic processes that could modulate the biological impacts of reduced seawater pH.

Evidence of the outcome of community adjustment (either physiological or demographic) to the effects of ocean acidification on NCC was limited in our study, as has been reported previously (Dove et al. 2013, 2020; Comeau et al. 2019), although one case of acclimation has been described (McLachlan et al. 2022). While NCC changed over time for both communities (Table 1), these effects appeared stochastic rather than directional outcomes reflecting an attenuated response. This interpretation is consistent with the absence of seasonal variation in the NCC-NCP relationships (Fig. 2). Community adjustment to ocean acidification would require time for acclimatization to occur, or to allow for changes in abundance of coral colonies based on susceptibility to changing conditions. Therefore, it is reasonable to expect these outcomes to be gradually expressed as the experiments progressed, thus favoring changes in the NCP-NCC relationships later in the year-long incubations (Fig. 2). The influence of coral reef community composition on the NCP-NCC relationship (Koweek et al. 2015) provides a rationale to expect change in these relationships, but the absence of these effects (Fig. 2) is inconsistent with this expectation (although they do not refute it). Overall, the only evidence that the present reef communities changed their sensitivity to ocean acidification comes from the fore reef communities, for which the sensitivity of 24-h NCC to $p\text{CO}_2$ increased (Hypothesis 2, Fig. 3). Based on a contrast of the slopes of 24-h NCC vs. $p\text{CO}_2$ in the final vs. the initial month, the sensitivity to $p\text{CO}_2$ increased by 55% (Fig. 3), most likely because of mortality of massive *Porites* (Edmunds et al. 2020). Massive *Porites* is less sensitive to ocean acidification than *Acropora* spp. (Comeau et al. 2014), which had become relatively more abundant in the fore reef communities towards the end of the experiment.

Hypothesis 3: Effects of ocean acidification on the NCP-NCC relationship

The inorganic-organic balance of carbon sequestration, expressed as the slope of NCP-NCC relationships, was not significantly different between $p\text{CO}_2$ treatments in both the fore reef and back reef communities (Fig. 2). However, the NCP-NCC slopes for the back reef communities were higher than those for the fore reef, indicating ecosystem metabolism operated at a higher rate in back reef communities (Falter et al. 2013). This likely is due to higher PFD for back reef communities that drive NPP to stimulate NCC, either through energetic contributions, or through altered intracellular pH favoring calcification. However, in both our experiments, the major difference in NCP-NCC relationships among treatments was a decrease in elevation that reflected the effects of lower seawater pH on NCC, but not NCP.

Treatment conditions

Because temperature varied seasonally in our experiment, the potential was created for interactive effects with ocean acidification, for example, with the stimulatory effects of temperature on calcification (Pratchett et al. 2015) attenuating the inhibitory effects of high $p\text{CO}_2$. Such effects were not evident at 564 μatm or 762–782 μatm $p\text{CO}_2$ (Fig. 1), and at 1067–1433 μatm $p\text{CO}_2$ were weakly expressed around March–April before suppression of NCC for the rest of the year.

The $p\text{CO}_2$ in the ambient flumes varied over the year, probably through temperature-related changes in the $p\text{CO}_2$ of the seawater with which the flumes were continually filled. These effects would have been augmented by the metabolism of the communities, which modifies seawater $p\text{CO}_2$ through respiration and photosynthesis. The two to three flumes in which $p\text{CO}_2$ was adjusted dynamically maintained distinct treatments effects (Supporting Information Table S1), which were similar between experiments and created treatments levels expected to occur under RCP8.5 by about 2053 (564 μatm $p\text{CO}_2$), 2080 (762–782 μatm $p\text{CO}_2$), or from 2095 to 2151 (1067–1433 μatm $p\text{CO}_2$) (IPCC 2014). The mean $p\text{CO}_2$ in the flumes resulted in back reef communities being incubated at an Ω_{arag} of 3.86 (ambient), 2.94 (564 μatm $p\text{CO}_2$), 2.45 (762 μatm $p\text{CO}_2$), or 1.85 (1067 μatm $p\text{CO}_2$), and fore reef communities being incubated at an Ω_{arag} of 3.83 (ambient), 2.45 (782 μatm $p\text{CO}_2$), or 1.53 (1433 μatm $p\text{CO}_2$).

Integrated PFD for the back reef communities was low ($16.3 \pm 0.4 \text{ mol photons m}^{-2} \text{ d}^{-1}$, averaged over time and among flumes) relative to the long-term, integrated PFD estimated for 2-m depth ($33.9 \pm 0.5 \text{ mol photons m}^{-2} \text{ d}^{-1}$, $n = 452$ d) using K_{dPAR} calculated from PAR measured at 17-m depth on the fore reef of Moorea (PJ Edmunds unpublished data). However, integrated PFD for the fore reef communities ($5.4 \pm 0.5 \text{ mol photons m}^{-2} \text{ d}^{-1}$) was similar to the long-term integrated PFD at 17-m depth ($8.1 \pm 0.2 \text{ mol photons m}^{-2} \text{ d}^{-1}$, $n = 454$ d). The low integrated PFD during the back reef

incubations might be a consequence of the narrow flumes in restricting light at low sun angles.

While low integrated PFD raises the possibility that NCP in the back reef experiment was underestimated because of sub-saturating light for photosynthesis (cf Takahashi et al. 2016), this effect probably was small since net photosynthesis of these communities saturates at $\sim 300 \mu\text{mol photons m}^{-2} \text{ s}^{-1}$ (Comeau et al. 2017). Likewise, since NCC for the back reef under ambient conditions (~ 80 –120 $\text{mmol CaCO}_3 \text{ m}^{-2} 24 \text{ h}^{-1}$, equivalent to ~ 8 –10 g $\text{CaCO}_3 \text{ m}^{-2} 24 \text{ h}^{-1}$, Fig. 1) is similar to NCC under ambient conditions for back reef ($\sim 3.8 \text{ g CaCO}_3 \text{ m}^{-2} 24 \text{ h}^{-1}$) and fore reef (~ 5 –10 g $\text{CaCO}_3 \text{ m}^{-2} 24 \text{ h}^{-1}$) communities at Heron Island (Dove et al. 2013, 2020), yet is higher than in situ measurements from the back reef of Moorea in 2018 ($\sim 42 \text{ mmol CaCO}_3 \text{ m}^{-2} 24 \text{ h}^{-1}$, Doo et al. 2019), it is unlikely that low integrated PFD downwardly biased the present estimates of NCC.

Ocean acidification impacts on inorganic and organic cycling of carbon in a reef community

The slope of NCP vs. NCC did not differ among $p\text{CO}_2$ treatments for both communities, but they were less steep for the back reef compared to the fore reef (Fig. 2). The steeper slope of the NCP-NCC relationship for the fore reef suggests that there is more deposition of CaCO_3 for every unit of organic carbon sequestered through photosynthesis. Such an increase in slope of the NCP-NCC relationship is generally observed for reefs with larger NCP ranges (e.g., Cyronak et al. 2018), where the elevation of day-time seawater pH increases benthic calcification (e.g., DeCarlo et al. 2017). Coral reefs on which both the cover of coral and macroalgae is elevated can calcify at high rates because photosynthesis by macroalgae draws down seawater CO_2 thus increasing day-time pH and seawater Ω_{arag} (DeCarlo et al. 2017).

In both communities, increased $p\text{CO}_2$ depressed the elevation of the linear relationships between NCC and NCP, suggesting that $p\text{CO}_2$ impairs the capacity for photosynthesis to support calcification; this effect was larger for the fore reef (Fig. 2). The elevation of these relationships declined 54% at the highest compared to ambient $p\text{CO}_2$ for the back reef (but remained positive at the intercept), whereas for the fore reef, it declined from $0.88 \text{ mmol CaCO}_3 \text{ m}^{-2} \text{ h}^{-1}$ to $-0.19 \text{ mmol CaCO}_3 \text{ m}^{-2} \text{ h}^{-1}$ (i.e., gross dissolution) at the intercept. The high abundance of carbonate sediment in the back reef, but not in the fore reef community, might account for these effects. Previous experimental studies of coral reef community metabolism, which have included sediments in the experimental design, have reported amelioration of the effects of ocean acidification relative to those expected in a reef lacking sediments (e.g., Dove et al., 2013; Doo et al. 2019; Dove et al., 2020). This trend suggests that a reef containing sediment-dominated habitats might be more resistant to the negative consequences of ocean acidification on calcification (vs. rubble dominated habitats). Other studies employing in

situ approaches have reported negative impacts of ocean acidification on coral reef sediments, with net dissolution initiated at an Ω_{arag} of 2.92 (Eyre et al. 2018). The contrasting results from our study might reflect two features of our experimental incubation that cannot currently be distinguished. First, it is possible that the 3-dimensional reef biota could enhance flow around and over branching corals (Monismith 2007), which would reduce flow across sediment surfaces in between them, and depress the advective exchange of solutes between sediments and overlying seawater (Santos et al. 2010). Second, the sand in our sediment boxes was prepared with flat surfaces, and lacked the surface ripples that characterize areas of reef sediment and enhance advective exchange with overlying seawater (Huettel et al. 2014). However, in the back reef communities, holothurians incubated within flumes would likely bioturbate carbonate sediments through feeding, potentially increasing dissolution signals (Vidal-Ramirez and Dove 2016), and within the framework of ocean acidification scenarios from our study, could facilitate buffering effects through increased omega saturation.

Back reef vs. fore reef

The coral reef communities we studied are representative of back reef and fore reef communities throughout French Polynesia (Vercelloni et al. 2019), and are similar to those occurring throughout tropical central and western Pacific (Moritz et al. 2018). Because we completed experiments with different communities from contrasting habitats, the incubations for each community were completed under unique but ecologically relevant environmental conditions. The communities also were composed of benthic space holders differing in identity as well as relative and absolute abundance (Edmunds et al. 2019a,b; 2020), although their cover similarly summed to $\sim 26\%$.

The coral taxa in the present communities grow at different rates (Pratchett et al. 2015), and the mechanisms determining the dissolution of sand and reef rock at reduced pH are unlikely to be the same (Andersson and Gledhill 2013; Comeau et al. 2016). Therefore, it was reasonable to expect that back reef and fore reef communities would respond in different ways to ocean acidification. This expectation was supported (Fig. 1), with the highest $p\text{CO}_2$ regime associated with dissolution (i.e., for 24-h NCC) of the fore reef (but not the back reef) within 4 months of exposure to the treatments. This effect was largely a result of nocturnal dissolution (night-NCC). A prominent role of nocturnal dissolution in the fore reef at high $p\text{CO}_2$ is consistent with previous studies (Dove et al. 2013, 2020), and underscores the role of carbonate dissolution at low pH within reef rock (cf Andersson and Gledhill 2013; Comeau et al. 2015) that occupied 53% of the benthic space when the experiment began. Because it is reasonable to suggest that the limited dissolution in the back reef at high $p\text{CO}_2$ was associated with the high cover (60%) of sediment (cf the fore reef) (described above), it might be

interesting to further explore the role of sediment porosity and surface rippling in mediating reef dissolution.

Summary

This study tested for the effects of ocean acidification on the metabolism of coral communities. We extended the frontier of ecological relevance of ocean acidification research on coral reefs by conducting year-long experiments with large areas of reef communities incubated under unidirectional flow in outdoor flumes, where temperature and light tracked ambient conditions. Response variables reflecting community metabolism and reef ecology were used to test our three hypotheses, and to close the gap between ocean acidification research on coral reefs and the ecological field that has quantified the coral reef crisis (Hughes et al. 2018).

Our results reveal the negative consequences of ocean acidification for coral reefs that remain hidden beneath a patina of ecological dynamics that is likely to remain indistinguishable from that of communities exposed to current ambient $p\text{CO}_2$. Beneath the living surface of coral reefs, ocean acidification pushes reef metabolism into net dissolution, with enhancement of this effect in deeper fore reef communities threatening to undermine the structural integrity of the reef framework. The possibility that reef communities might avoid being undermined by dissolution at high $p\text{CO}_2$ through “adjustments” to lessen the effects of ocean acidification is not supported by the present study, but we recognize that our study cannot refute this possibility (i.e., it may occur but is not detected by the methods we employed). Our results suggest it would be unwise to project the structure and function of coral reefs in a more acidic future by assuming that their sensitivity to ocean acidification will be any different from what currently is known from existing studies.

Data availability statement

The data supporting this manuscript are archived at Dryad: doi.org/10.5061/dryad.00000009d.

References

- Albright, R., and others. 2016. Reversal of ocean acidification enhances net coral reef calcification. *Nature* **531**: 362–365. doi:10.1038/nature17155
- Andersson, A. J., and D. Gledhill. 2013. Ocean acidification and coral reefs: Effects on breakdown, dissolution, and net ecosystem calcification. *Ann. Rev. Mar. Sci.* **5**: 321–348. doi:10.1146/annurev-marine-121211-172241
- Burgess, S. C., E. C. Johnston, A. S. J. Wyatt, J. J. Leichter, and P. J. Edmunds. 2021. Response diversity in corals: Hidden differences in bleaching mortality among cryptic *Pocillopora* species. *Ecology* **102**: e03324. doi:10.1002/ecy.3324
- Camp, E. F., and others. 2020. Corals exhibit distinct patterns of microbial reorganisation to thrive in an extreme inshore

environment. *Coral Reefs* **39**: 701–716. doi:10.1007/s00338-019-01889-3

Carpenter, R. 2023. MCR LTER: Coral reef: Long-term population and community dynamics: Benthic algae and other community components, ongoing since 2005. Environmental Data Initiative. doi:10.6073/pasta/840b2f0f38b3f8546d2b2f6d3ab3a0d5

Carpenter, R. C., C. A. Lantz, E. Shaw, and P. J. Edmunds. 2018. Responses of coral reef community metabolism in flumes to ocean acidification. *Mar. Biol.* **165**: 66. doi:10.1007/s00227-018-3324-0

Clark, M. S. 2020. Molecular mechanisms of biomineralization in marine invertebrates. *J. Exp. Biol.* **223**: jeb206961. doi:10.1242/jeb.206961

Comeau, S., P. J. Edmunds, N. B. Spindel, and R. C. Carpenter. 2014. Diel $p\text{CO}_2$ oscillation modulates the response of the coral *Acropora hyacinthus* to ocean acidification. *Mar. Ecol. Prog. Ser.* **501**: 99–111. doi:10.3354/meps10690

Comeau, S., R. C. Carpenter, C. A. Lantz, and P. J. Edmunds. 2015. Ocean acidification accelerates dissolution of experimental coral reef communities. *Biogeosciences* **12**: 365–372. doi:10.5194/bg-12-365-2015

Comeau, S., C. A. Lantz, P. J. Edmunds, and R. C. Carpenter. 2016. Framework of barrier reefs threatened by ocean acidification. *Glob. Change Biol.* **22**: 1225–1234. doi:10.1111/gcb.13023

Comeau, S., E. Tambutté, R. C. Carpenter, P. J. Edmunds, N. R. Evensen, D. Allemand, G. Ferrier-Pagès, S. Tambutté, and A. A. Venn. 2017. Coral calcifying fluid pH is modulated by seawater carbonate chemistry not solely seawater pH. *Proc. Royal. Soc. B.* **284**: 20161669. doi:10.1098/rspb.2016.1669

Comeau, S., C. E. Cornwall, T. M. DeCarlo, S. S. Doo, R. C. Carpenter, and M. T. McCulloch. 2019. Resistance to ocean acidification in coral reef taxa is not gained by acclimatization. *Nat. Clim. Change* **9**: 477–483. doi:10.1038/s41558-019-0486-9

Cornwall, C. E., C. D. Heptburn, C. A. Pilditch, and C. Hurd. 2013. Concentration boundary layers around complex assemblages of macroalgae: Implications for the effects of ocean acidification on understory coralline algae. *Limnol. Oceanogr.* **58**: 121–130. doi:10.4319/lo.2013.58.1.0121

Cornwall, C. E., and others. 2021. Global declines in coral reef calcium carbonate production under ocean acidification and warming. *Proc. Natl. Acad. Sci. U. S. A.* **118**: e2015265118. doi:10.1073/pnas.2015265118

Cyronak, T., and others. 2018. Taking the metabolic pulse of the world's coral reefs. *PLoS One* **13**: e0190872. doi:10.1371/journal.pone.0190872

DeCarlo, T. M., A. L. Cohen, G. T. F. Wong, F.-K. Shiah, A. J. Lentz, K. A. Davis, K. E. F. Shamburger, and P. Lohmann. 2017. Community production modulates coral reef pH and the sensitivity of ecosystem calcification to ocean acidification. *J. Geophys. Res. Oceans* **122**: 745–761. doi:10.1002/2016JC012326

Dickson, A. G., C. L. Sabine, and J. R. Christian [eds.]. 2007. Guide to best practices for ocean CO_2 measurements, v. 3. PICES Special Publication, p. 191.

Doney, S. C., V. J. Fabry, R. A. Feely, and J. A. Kleypas. 2009. Ocean acidification: The other CO_2 problem. *Ann. Rev. Mar. Sci.* **1**: 169–192. doi:10.1146/annurev.marine.010908.163834

Doo, S. S., P. J. Edmunds, and R. C. Carpenter. 2019. Ocean acidification effects on *in situ* coral reef metabolism. *Sci. Rep.* **9**: 12067. doi:10.1038/s41598-019-48407-7

Doo, S. S., A. Leplastrier, A. Graba-Laundry, J. Harianto, R. A. Coleman, and M. Byrne. 2020. Amelioration of ocean acidification and warming effects through physiological buffering of a macroalgae. *Ecol. Evol.* **10**: 8465–8475. doi:10.1002/ece3.6552

Dove, S. G., D. I. Kline, O. Pantos, F. E. Angly, G. W. Tyson, and O. Hoegh-Guldberg. 2013. Future reef decalcification under a business-as-usual CO_2 emission scenario. *Proc. Natl. Acad. Sci. U. S. A.* **110**: 15342–15347. doi:10.1073/pnas.1302701110

Dove, S. G., K. T. Brown, A. Van Den Heuvel, A. Chai, and O. Hoegh-Guldberg. 2020. Ocean warming and acidification uncouple calcification from calcifier biomass which accelerates coral reef decline. *Commun. Earth Environ.* **1**: 55. doi:10.1038/s43247-020-00054-x

Edmunds, P. 2024. MCR LTER: Coral Reef: Long-term Population and Community Dynamics: Corals, ongoing since 2005 ver 40. Environmental Data Initiative. doi:10.6073/pasta/15d5120fb4f7b79811b16287eae15a35

Edmunds, P. J., and others. 2016. Integrating the effects of ocean acidification across functional scales on tropical coral reefs. *Biosciences* **66**: 350–362. doi:10.1093/biosci/biw023

Edmunds, P. J., S. S. Doo, and R. C. Carpenter. 2019a. Changes in coral reef community structure in response to year-long incubations under contrasting $p\text{CO}_2$ regimes. *Mar. Biol.* **166**: 94. doi:10.1007/s00227-019-3540-2

Edmunds, P. J., T. C. Adam, A. C. Baker, S. S. Doo, P. W. Glynn, D. P. Manzello, N. J. Silbiger, T. B. Smith, and P. Fong. 2019b. Why more comparative approaches are required in time-series analyses of coral reef ecosystems. *Mar. Ecol. Prog. Ser.* **608**: 287–306. doi:10.3354/meps12805

Edmunds, P. J., S. S. Doo, and R. C. Carpenter. 2020. Year-long effects of high $p\text{CO}_2$ on the community structure of a tropical fore reef assembled in outdoor flumes. *ICES J. Mar. Sci.* **77**: 1055–1065. doi:10.1093/icesjms/fsaa015

Eyre, B. D., T. Cyronak, P. Drupp, E. H. De Carlo, J. P. Sachs, and A. J. Andersson. 2018. Coral reefs will transition to net dissolving before end of century. *Science* **359**: 908–911. doi:10.1126/science.aoa1118

Falter, J. L., R. J. Lowe, Z. Zhang, and M. McCulloch. 2013. Physical and biological controls on the carbonate chemistry of coral reef waters: Effects of metabolism, wave forcing, sea level, and geomorphology. *PLoS One* **8**: e53303. doi:10.1371/journal.pone.0053303

Fantazzini, P., and others. 2015. Gains and losses of coral skeletal porosity changes with ocean acidification acclimation. *Nat. Commun.* **6**: 7785. doi:[10.1038/ncomms8785](https://doi.org/10.1038/ncomms8785)

Findlay, H. S., and C. Turley. 2021. Ocean acidification and climate change, p. 251–279. In T. M. Letcher [ed.], *Climate change: Observed impacts on planet earth*, Third ed. Elsevier.

Hench, J. L., J. J. Leichter, and S. G. Monismith. 2008. Episodic circulation and exchange in a wave-driven coral reef and lagoon system. *Limnol. Oceanogr.* **53**: 2681–2694. doi:[10.4319/lo.2008.53.6.2681](https://doi.org/10.4319/lo.2008.53.6.2681)

Hoegh-Guldberg, O., and others. 2007. Coral reefs under rapid climate change and ocean acidification. *Science* **318**: 1737–1742. doi:[10.1126/science.1152509](https://doi.org/10.1126/science.1152509)

Hofmann, G. E., J. P. Barry, P. J. Edmunds, R. D. Gates, D. A. Hutchins, T. Klinger, and M. A. Sewell. 2010. The effect of ocean acidification on calcifying organisms in marine ecosystems: An organism-to-ecosystem perspective. *Annu. Rev. Ecol. Evol. Syst.* **41**: 127–147. doi:[10.1146/annurev.ecolsys.110308.120227](https://doi.org/10.1146/annurev.ecolsys.110308.120227)

Hofmann, G. E., and others. 2011. High-frequency dynamics of ocean pH: A multi-ecosystem comparison. *Plos One* **6**: e28983. doi:[10.1371/journal.pone.0028983](https://doi.org/10.1371/journal.pone.0028983)

Huettel, M., J. E. Berg, and J. E. Kostka. 2014. Benthic exchange and biogeochemical cycling in permeable sediments. *Ann. Rev. Mar. Sci.* **6**: 23–51. doi:[10.1146/annurev-marine-051413-012706](https://doi.org/10.1146/annurev-marine-051413-012706)

Hughes, T. P., and others. 2018. Global warming transforms coral reef assemblages. *Nature* **556**: 492–496. doi:[10.1038/s41586-018-0041-2](https://doi.org/10.1038/s41586-018-0041-2)

IPCC. 2018. Global warming of 1.5°C. An IPCC special report on the impacts of global warming of 1.5°C above pre-industrial levels and related global greenhouse gas emission pathways, in the context of strengthening the global response to the threat of climate change, sustainable development, and efforts to eradicate poverty. Cambridge Univ. Press, p. 616. doi:[10.1017/9781009157940](https://doi.org/10.1017/9781009157940)

Kowek, D., R. B. Dunbar, J. S. Rogers, G. J. Williams, N. Price, D. Mucciarone, and L. Teneva. 2015. Environmental and ecological controls of coral community metabolism on Palmyra atoll. *Coral Reefs* **34**: 339–351. doi:[10.1007/s00338-014-1217-3](https://doi.org/10.1007/s00338-014-1217-3)

Kroeker, K. J., R. L. Kordas, R. N. Crim, and G. G. Singh. 2010. Meta-analysis reveals negative yet variable effects of ocean acidification on marine organisms. *Ecol. Lett.* **13**: 1419–1434. doi:[10.1111/j.1461-0248.2010.01518.x](https://doi.org/10.1111/j.1461-0248.2010.01518.x)

Kroeker, K. J., R. I. Kordas, R. Crim, I. E. Hendriks, L. Ramajo, G. S. Singh, C. M. Duarte, and J. P. Gattuso. 2013. Impacts of ocean acidification on marine organisms: Quantifying sensitivities and interaction with warming. *Glob. Change Biol.* **19**: 1884–1896. doi:[10.1111/gcb.12179](https://doi.org/10.1111/gcb.12179)

Langdon, C., T. Takahashi, C. Sweeney, D. Chipman, J. Goddard, F. Marubini, H. Aceves, H. Barnett, and M. J. Atkinson. 2000. Effect of calcium carbonate saturation state on the calcification rate of an experimental coral reef. *Global Biogeochem. Cycles* **14**: 639–654. doi:[10.1029/1999GB001195](https://doi.org/10.1029/1999GB001195)

Langdon, C., and M. J. Atkinson. 2005. Effect of elevated $p\text{CO}_2$ on photosynthesis and calcification of corals and interactions with seasonal change in temperature/irradiance and nutrient enrichment. *J. Geophys. Res. Oceans* **110**: 1–16. doi:[10.1029/2004JC002576](https://doi.org/10.1029/2004JC002576)

Lavigne, H., and J.-P. Gattuso. 2013. Seacarb: seawater carbonate chemistry with R. R package version 2.4.10, <http://CRAN.R-project.org/package=seacarb>

McLachlan, R. H., J. T. Price, A. Muñoz-Garcia, N. L. Weisleder, S. J. Levas, C. P. Jury, R. J. Toonen, and A. G. Grottoli. 2022. Physiological acclimatization in Hawaiian corals following a 22-month shift in baseline seawater temperature and pH. *Sci. Rep.* **12**: 3712. doi:[10.1038/s41598-022-06896-z](https://doi.org/10.1038/s41598-022-06896-z)

Monismith, S. G. 2007. Hydrodynamics of coral reefs. *Annu. Rev. Fluid Mech.* **39**: 37–55. doi:[10.1146/annurev.fluid.38.050304.092125](https://doi.org/10.1146/annurev.fluid.38.050304.092125)

Moritz, C., J. Vii, W. L. Long, J. Tamelander, A. Thomassin, and S. Planes [eds.]. 2018. Status and trends of coral reefs of the Pacific. Global Coral Reef Monitoring Network.

Moss, R. H., and others. 2010. The next generation of scenarios for climate change research and assessment. *Nature* **463**: 747–756. doi:[10.1038/nature08823](https://doi.org/10.1038/nature08823)

Pratchett, M. S., K. D. Anderson, M. O. Hoogenboom, E. Widman, A. Baird, J. M. Pandolfi, P. J. Edmunds, and J. M. Lough. 2015. Spatial, temporal and taxonomic variation in coral growth—implications for the structure and function of coral reef ecosystems. *Oceanogr. Mar. Biol. Ann. Rev.* **53**: 215–285.

Putnam, H. M., J. M. Davidson, and R. D. Gates. 2016. Ocean acidification influences host DNA methylation and phenotypic plasticity in environmentally susceptible corals. *Evol. Appl.* **9**: 1165–1178. doi:[10.1111/eva.12408](https://doi.org/10.1111/eva.12408)

Riebesell, U., and J. P. Gattuso. 2015. Lessons learned from ocean acidification research. *Nat. Clim. Change* **5**: 12–14. doi:[10.1038/nclimate2456](https://doi.org/10.1038/nclimate2456)

Santos, I. R., D. Erler, D. Tait, and B. D. Eyre. 2010. Breathing of a coral cay: Tracing tidally driven seawater recirculation in permeable coral reef sediments. *J. Geophys. Res.* **115**: C12010. doi:[10.1029/2010JC006510](https://doi.org/10.1029/2010JC006510)

Schoepf, V., C. P. Jury, R. J. Toonen, and M. T. McCulloch. 2017. Coral calcification mechanisms facilitate adaptive responses to ocean acidification. *Proc. Royal. Soc. B.* **284**: 2017–2117. doi:[10.1098/rspb.2017.2117](https://doi.org/10.1098/rspb.2017.2117)

Smith, S. V. 1973. Carbon dioxide dynamics: A record of organic carbon production, respiration, and calcification in the Eniwetok windward reef flat community. *Limnol. Oceanogr.* **18**: 106–120.

Takashita, Y., W. McGillis, E. M. Briggs, A. L. Carter, E. M. Donham, T. R. Martz, N. N. Price, and J. E. Smith. 2016. Assessment of net community production and calcification of a coral reef using a boundary layer approach. *J. Geophys. Res. Oceans* **121**: 5655–5671. doi:[10.1002/2016JC011886](https://doi.org/10.1002/2016JC011886)

Vercelloni, J., M. Kayal, Y. Chancerelle, and S. Planes. 2019. Exposure, vulnerability, and resiliency of French Polynesian coral reefs to environmental disturbances. *Sci. Rep.* **9**: 1027. doi:10.1038/s41598-018-38228-5

Veron, J. E. N. 2000. *Corals of the world* vol 1–3. Australian Institute of Marine Science. Townsville MC.

Vidal-Ramirez, F., and S. Dove. 2016. Diurnal effects of *Holothuria atra* on seawater carbonate chemistry in a sedimentary environment. *J. Exp. Mar. Biol. Ecol.* **474**: 156–161.

Washburn, L., and Moorea Coral Reef LTER. 2023. MCR LTER: Coral reef: Ocean currents and biogeochemistry: Salinity, temperature and current at CTD and ADCP mooring FOR01 from 2004 ongoing ver 40. Environmental Data Initiative.

Reef LTER (OCE 16-37396), and it benefitted from gifts from the Gordon and Betty Moore Foundation. The research was conducted under permits issued by the Government of French Polynesia (Délégation à la Recherche) and the Haut-commissariat de la République en Polynésie Française (DTRT) (Protocole d'Accueil 2015–2018). The 2 years of experiments were conducted with the support of many people, including our technical staff, N. Spindel, C. Lantz, and G. Srednick, and numerous graduate students. We thank S. Comeau for inspiration in designing the flumes, and N. Davies and the staff of the Richard B Gump South Pacific Research Station for making our visits to Moorea productive and enjoyable. This is contribution number 382 of the CSUN marine biology program.

Conflict of Interest

None declared.

Submitted 08 June 2023

Revised 08 December 2023

Accepted 25 December 2023

Associate editor: Bradley D. Eyre

Acknowledgments

This research was supported by the US National Science Foundation through grants to PJE and RCC (OCE 14-15268) and the Moorea Coral